A Study of the Effect of Sintering Conditions of $Mg_{0.95}Ni_{0.05}Ti_3$ on Its Physical and Dielectric Properties

Chun-Hsu Shen [1], Chung-Long Pan [2] and Shih-Hung Lin [1,*]

[1] Department of Electronic Engineering, National Yunlin University of Science and Technology, Yunlin 64002, Taiwan; jameschs@yuntech.edu.tw
[2] Department of Electrical Engineering, I-Shou University, Kaohsiung 84001, Taiwan; ptl@isu.edu.tw
*   Correspondence: isshokenmei@yuntech.edu.tw; Tel.: +886-05-5342601 (ext. 4344); Fax: +886-05-5312063

check for updates

Abstract: $Mg_{0.95}Ni_{0.05}TiO_3$ ceramics were prepared by traditional solid-state route using sintering temperatures between 1300 and 1425 °C and holding time of 2–8 h. The sintered samples were characterized for their phase composition, micro-crystalline structure, unit–cell constant, and dielectric properties. A two-phase combination region was identified over the entire compositional range. The effect of sintering conditions was analyzed for various properties. Both permittivity (ε_r) and Q factor (Q_f) were sensitive to sintering temperatures and holding times, and the optimum performance was found at 1350 °C withholding time of 4 h. The temperature coefficient of resonant frequency (τ_f) in a range from −45.2 to −52 (ppm/°C) and unit–cell constant were not sensitive to both the sintering temperature and holding time. An optimized Q factor of 192,000 (GHz) related with a permittivity (ε_r) of 17.35 and a temperature coefficient (τ_f) of −47 (ppm/°C) was realized for the specimen sintered at 1350 °C withholding time of 4 h. For applications of 5G communication device (filter, antennas, etc.), $Mg_{0.95}Ni_{0.05}TiO_3$ is considered to be a suitable candidate for substrate materials.

Keywords: microwave performances; sintering temperature; low-loss ceramics; $Mg_{0.95}Ni_{0.05}TiO_3$

1. Introduction

Due to the speedy evolution of communication technology, today's 5G, and even the next generation of communication systems, component performance improvement and size reduction are currently the first two goals. Therefore, to be able to effectively reduce the size and improve the performance of components, quite a few laboratories place their attention on electronic ceramics. In the field of microwave (MW) dielectrics applications [1–8], electronic ceramics are subject to the following conditions:

1. High permittivity (ε_r): the ε_r is inversely related to the wavelength in dielectrics ($\lambda = \lambda_0/\sqrt{\varepsilon_r}$), so the component size can be effectively reduced.
2. High-quality factor (Q factor, Q_f): Q factors are inversely related to the dielectric loss (Q = 1/tanδ), so high Q factors can improve frequency selectivity and stability in MW components.
3. A temperature coefficient (τ_f) close to zero: A τ_f value close to zero ensures that component performance is not affected by external temperatures.

Magnesium titanium ($MgTiO_3$) is a member of the ilmenite group which crystallizes in the trigonal system [9–16]. $MgTiO_3$-based ceramics have been widely applied to dielectrics in resonators, filters, and antennas for communication, radar, and global positioning systems operated at microwave

frequencies. They have a fairly low dielectric loss (4.5×10^{-5}) and a minus temperature coefficient ($\tau_f = -50$ ppm/°C), when blending with $CaTiO_3$, which has a perovskite structure and extensive plus temperature coefficient (τ_f) ~ +800 ppm/°C. As blending ratio with 95:5, the combination was manifested a τ_f value ~ 0 ppm/°C, a permittivity (ε_r) ~ 21, and loss tan = 1.25×10^{-4} at 7 GHz [9,17–19]. However, because the sintering temperature (S.T.) of the phase combination is too high (up to 1450 °C), quite a lot of research has been done to effectively reduce its S.T. For example, improve the conditions of the process or add different sintering promoters. The dielectric performances of the combination can be further ameliorated by blending sintering addition such as Cr, La, or B [17–19].

The relevant research has pointed out that replacing magnesium with the 2 valence elements of 0.05 moles (such as Co^{2+}, Zn^{2+}), can get optimum characteristics [10,13,20]. With the partial replacement of Mg by Ni, $(Mg_{0.95}Ni_{0.05})TiO_3$ (MNT) ceramics with an ilmenite-type structure has been reported to possess excellent dielectric properties with a dielectric constant (ε_r) of 17.2, a quality factor ($Q \times f$ value) of 180,000 (GHz), and a temperature coefficient of resonant frequency (τ_f) ~ −45 ppm/°C) [10]. In the past, many researches manifested that MNT blended with positive temperature coefficient material (such as $CaTiO_3$, $SrTiO_3$, $Ca_{0.8}Sr_{0.2}TiO_3$, etc.) can be effectively reached close to zero temperature coefficient [20–22]. However, no studies have explored the characteristics of the pure MNT phase in depth until now. Therefore, we only know about the mixed-phase characteristics of MNT with blending positive τ_f materials. In this article, we try to supersede magnesium (Mg^{2+}: 0.072 nm) with trace amounts of nickel (Ni^{2+}: 0.069 nm). Magnesium (Mg^{2+}) superseded by nickel (Ni^{2+}) of 0.05 mole can enhance the densification of microstructure and microwave performances in the phase of MNT. The combination of MNT phase was combined by a solid-state method. The relevant microwave dielectric performances were analyzed according to the densification, X-ray Diffraction (XRD) analysis, unit–cell constant, and microstructure of the phase ((Scanning Electron Microscope (SEM) and Energy Dispersive Spectroscopy (EDS)) The connection between sintering conditions and microwave performances is also further discussed in the pure MNT phase.

2. Results and Discussion

XRD analysis of MNT phase combination at varied S.T. (1300 °C–1425 °C) and holding time (2–8 h) are shown in Figures 1 and 2, individually.
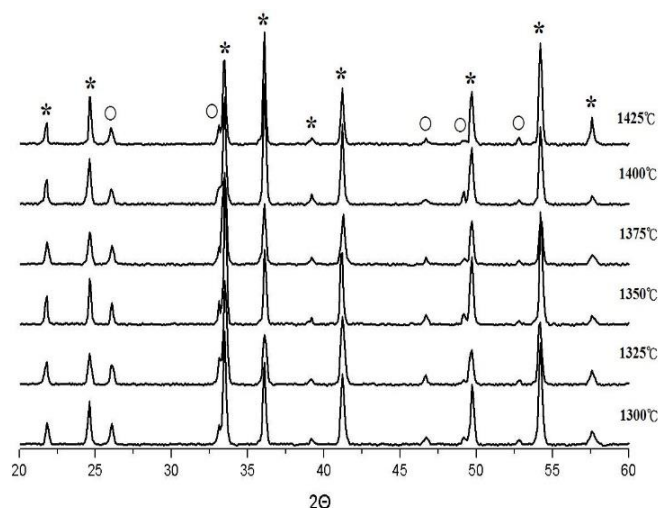

Figure 1. XRD analysis of MNT ceramics sintered at varied temperature holding times of 4 h. (*: MNT, ○: MNT2).

The MNT phase has an ilmenite-type structure, which is duplicated as magnesium titanium in the trigonal system (ICDD #06-0494). In this combination, MNT can be designated as the primary phase and a small fraction of the secondary phase $Mg_{0.95}Ni_{0.05}Ti_2O_5$ (MNT2 hereafter) existence.

The MNT2 was duplicated as $MgTi_2O_5$ (JCPDS File No. 82-1125), which usually appears at MgO and TiO_2 respond in a 1:2 mole ratio and is difficult to exhaustively remove in traditional solid-state reactions [23,24]. In this study, MNT2 was also designated as a secondary phase with permittivity (ε_r)~13.1, Q factor ~30,000 GHz, and τ_f ~−43 ppm/°C [25]. The microwave performance of the MNT phase may be diminished by the formation of the secondary phase. As expected, when the temperature rises, the ratio of the MNT2 phase rises because its growth conditions require a higher temperature of 1450 °C [25]. The relative percentage of MNT2 intensity raised from 10.4% to 13.2% as the S.T. raised from 1300 °C to 1425 °C. In contrast, this is also revealed at lower temperatures (<1450 °C), the proportion of the secondary phase will be less. Figure 2 shows that the same crystallization analysis results were held at 1350 °C for 2 to 8 h as mentioned above, with no significant change in both angle and intensity.
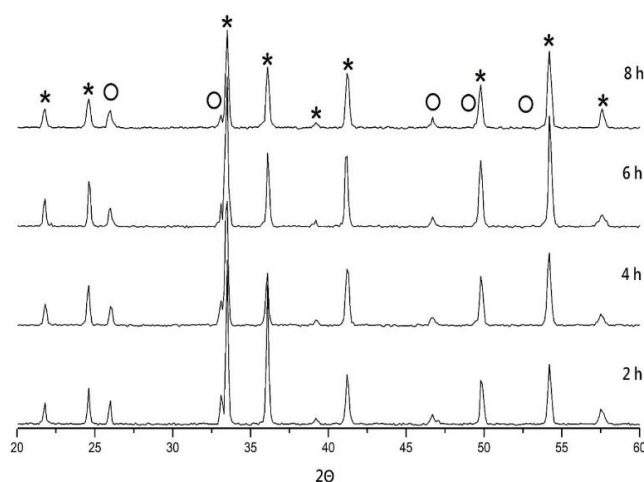

Figure 2. XRD analysis of MNT ceramics sintered at 1350 °C with varied holding time. (*: MNT, ◯: MNT2).

To further understand the structure and combination of the MNT phase, we have also calculated that the unit–cell constant of the MNT phase sintered at 1350 °C for a varied holding time as shown in Table 1. Compared with $MgTiO_3$ (ICDD-PDF #00-006-0494), the unit–cell constant of the MNT phase tended to decrease. The results showed that when 0.05 moles of nickel (Ni^{2+}) superseded magnesium (Mg^{2+}), a solid solution of the MNT phase could be formed. The change of MNT phase unit–cell constant was mainly since the ion radius of nickel (Ni^{2+}: 0.069 nm) is relatively smaller than that of magnesium (Mg^{2+}: 0.072 nm), which would lead to local changes in the unit–cell constant of MNT phase in a-site. This result indicates that when 0.05 mole nickel (Ni^{2+}) supersedes magnesium (Mg^{2+}) to form MNT phase, the unit–cell constant is reduced from (a = 0.5054, and c = 1.3898 nm) in $MgTiO_3$ to (a = 0.5046, and c = 1.3905 nm).

Table 1. The unit–cell constant of the MNT phase with varied holding times.

S.T.	Holding Time	a (nm)	c (nm)
1325 °C	2 h	0.5024 ± 0.00197	1.38518 ± 0.00398
	4 h	0.50395 ± 0.00100	1.38357 ± 0.00200
	6 h	0.50429 ± 0.00125	1.38971 ± 0.00254
1350 °C	2 h	0.50439 ± 0.00135	1.38850 ± 0.00273
	4 h	0.50459 ± 0.00126	1.39054 ± 0.00256
	6 h	0.50611 ± 0.00070	1.38949 ± 0.00141
1375 °C	2 h	0.50288 ± 0.00163	1.39250 ± 0.00335
	4 h	0.50386 ± 0.00080	1.38478 ± 0.00161
	6 h	0.50401 ± 0.00116	1.38811 ± 0.00235

To observe the growth of grains in crystalline structures, the surface microstructure photographs of MNT combinations at varied sintering conditions are shown in Figure 3a–f. It can be seen from the figure that at 1300 °C, the grains had not grown and the overall structure had not been compacted. The dimension of the grains rose with the rising of S.T., and it was more consistent to reach a highly uniform structure at 1350 °C. However, excessive S.T. (1400 °C) can lead to excessive grain expansion, which in turn can lead to an uneven arrangement in the structure and adversely affect the overall characteristics. Stick-like grain growth was enhanced as the S.T. higher than 1350 °C. This type of grain can be considered as MNT2 phase, the formation condition is that when the ratio of magnesium to titanium is 1:2, can be seen by the EDS analysis of Figure 4 (Spot C). MNT2 phases existed at higher temperatures as discussed earlier [26]. The EDS analysis of the specimen sintering at 1400 °C is also shown in Figure 4. It can be seen that the proportion of stick-like grain increases significantly at this S.T. Moreover, the microstructure of samples sintered at 1350 °C holding 2–6 h shown in Figure 3c,g,h sequentially revealed grains undergrown to overgrown process and well-grown grains was obtained at 1350 °C holding 4 h. As expected, MNT combinations were exhibited as primary phases associated with the apparent second phase MNT2 in the specimens. This was verified in the backscattered electronic (BEI) image shown in Figure 3h and EDS analysis in Figure 4.
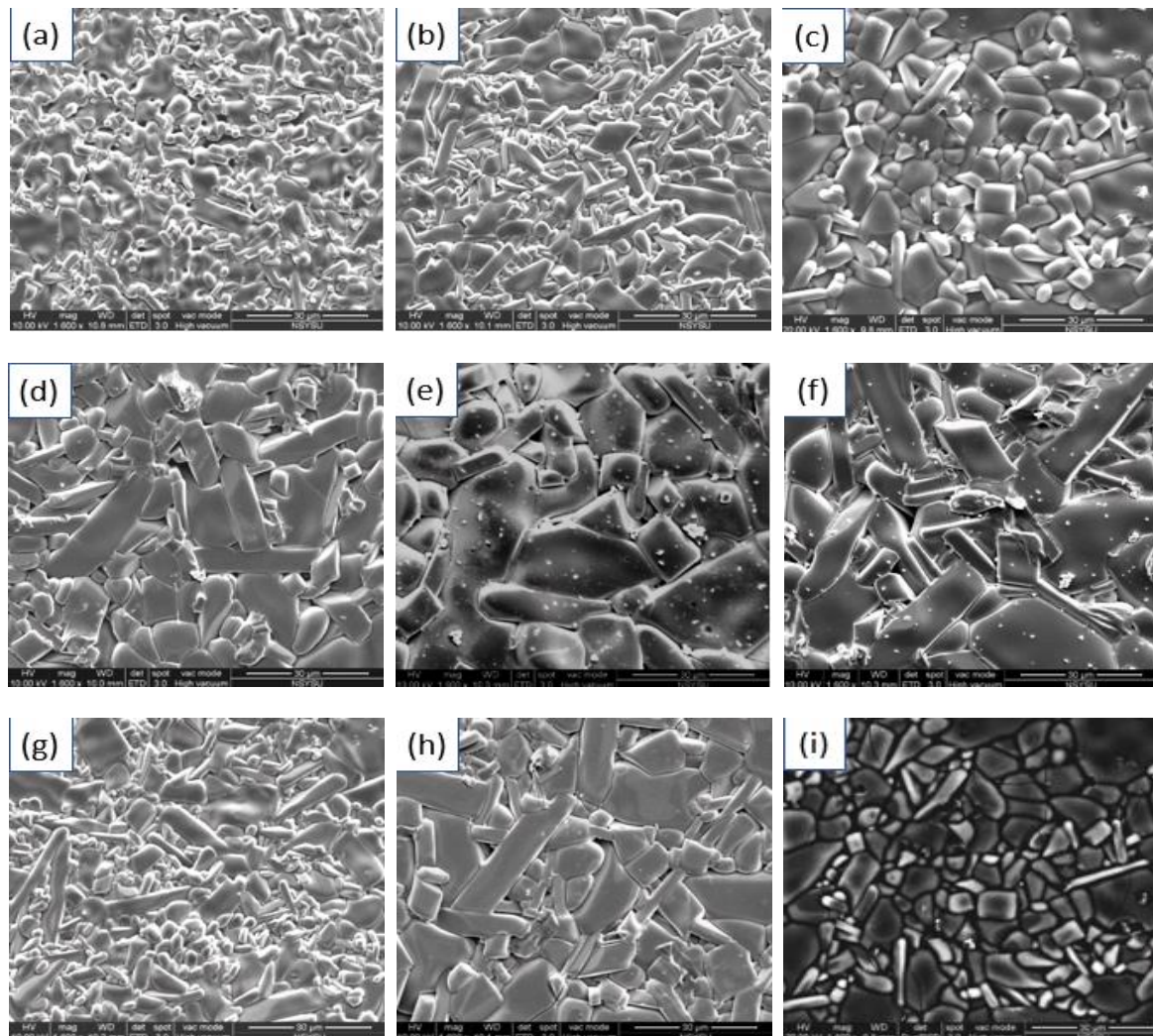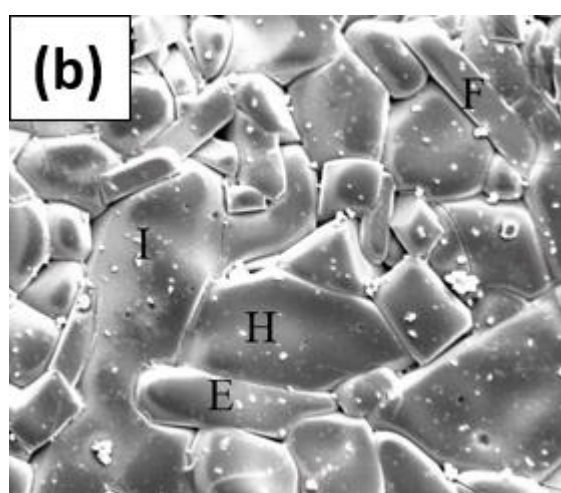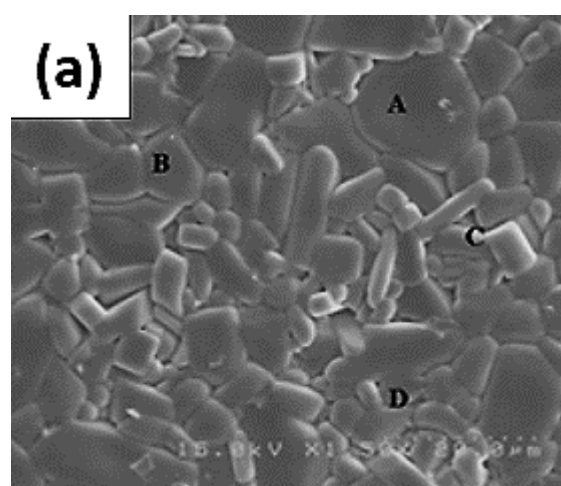

Figure 3. SEM photographs of MNT ceramics sintered at varied temperature holding times of 2–6 h and the BEI of MNT ceramics sintered at 1350 °C holding of 4 h: (**a**) 1300 °C; (**b**) 1325 °C; (**c**) 1350 °C; (**d**) 1375 °C; (**e**) 1400 °C; (**f**) 1425 °C; (**g**) 1350 °C/2 h; (**h**) 1300 °C/6 h; (**i**) BEI-1350 °C/4 h.

Spot	Atom(%)			
	MgK	**NiK**	**TiK**	**OK**
A	20.51	1.86	21.7	55.93
B	20.78	1.58	23.97	53.67
C	12.78	1.13	25.63	60.46
D	19.02	1.46	21.42	58.08
E	12.96	0.62	23.35	63.07
F	13.77	0.8	29.56	55.87
G	13.4	0.74	25.84	60.02
H	19.61	1.57	23.68	55.15
I	19.67	0.84	17.99	61.51

(c)

Figure 4. The EDS photographs of (**a**) MNT at 1350 °C (**b**) MNT2 at 1400 °C and (**c**) analysis of correspondent markings A–I.

Figure 5 shows the measured and relative densities of the MNT combinations sintered at varied temperatures holding 2–6 h. The optimum measured and relative densities of the MNT ceramics were 3.67 g/cm^3 and 94.3% inspected sintering at 1350 °C holding 4 h. The density of holding 4 h samples can be seen in the figure, reaching an optimal value as the S.T. rising to 1350 °C, and then showing a

downward trend as the temperature still goes up. The rise in density is mainly due to the expansion of grains, while the downward trend is due to the uneven structure caused by excessive grain growth as shown in Figure 3. On the other hand, a variation in the sintering holding time (2–4 h) would also expand the grains, resulting in an increment in the density as shown in Figure 3c,f. However, the density was also diminished with the longer holding time (6 h) caused by excessive grain growth shown in Figure 3g. The measured density and its proportional TD rose from 3.31 g/cm^3 (85.1% TD) to maximum values of 3.67 g/cm^3 (94.3%TD) as the S.T. rose from 1300 °C to 1350 °C for the MNT combinations with sintering holding 4 h.
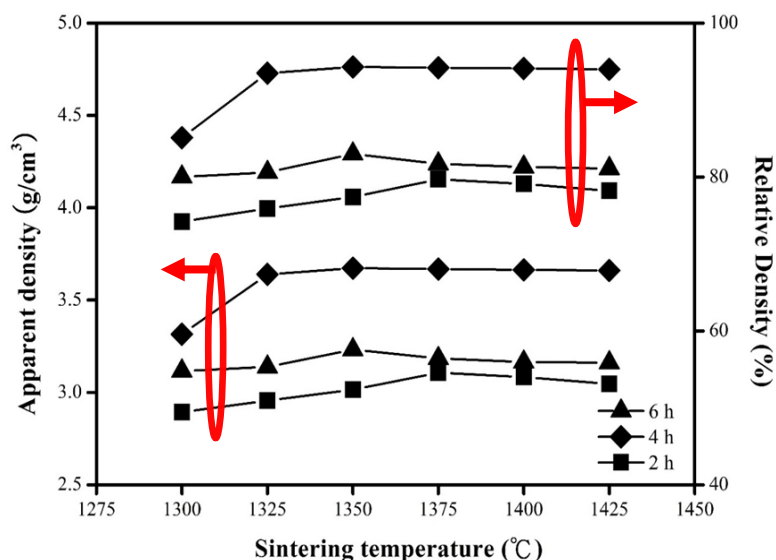

Figure 5. Dependence of apparent density and relative density on S.T. of the MNT ceramics for varied holding time. The left and right circles with arrows indicating apparent and relative density, respectively.

Figure 6 shows the results of permittivity (ε_r) and Q factors (Q_f) under different sintering conditions. The relationship between permittivity (ε_r) and the S.T. has an equivalent orientation as those among ionic polarization, relative density, and S.T. since higher density expresses lower porosity. When the S.T. went up, the permittivity (ε_r) rose slightly, and it can be found in the relevant literature that the permittivity (ε_r) in dielectric materials is mainly dominated by ion polarization [27]. As mentioned above, when nickel (Ni^{2+}) was superseded by magnesium (Mg^{2+}), the permittivity (ε_r) of MNT combinations descended. This may be because the replacement of nickel (Ni^{2+}) causes some compression in the unit–cell structure, which in turn deviates ionic polarization [28]. Therefore, the permittivity (ε_r) of MNT combinations is mainly determined by the ionic polarization. The relationship between the permittivity (ε_r) and S.T shows an identical tendency as that among density and S.T. because higher density results in lower porosity as shown in Figure 3. However, descended of permittivity (ε_r) was observed from 1375 °C holding 2 h. The rise in permittivity (ε_r) could be demonstrated owing to higher densities. Thus, rising S.T. does needless upshot in a higher permittivity (ε_r). The permittivity (ε_r) of the well-sintered MNT combinations ranged from 16.9 to 17.35 at 1300–1425 °C holding 4 h. An optimum permittivity (ε_r) of 17.35 was obtained for the MNT combinations sintered at 1350 °C holding 4 h.

The Q factor enhance with temperature rose to 1350 °C and then descended. An optimum Q factor of 192,000 (GHz) was acquired for MNT combinations at 1350 °C holding 4 h. The decline of the Q factors is mainly attributed to uneven structure due to excessive grain expansion at higher S.T., as shown in Figure 3. In general, the main causes of dielectric loss are the vibration mode of the unit–cell, pores, secondary phase, impurities, and structure defects [28]. As can be known from other relevant dielectric material performances, density is often one of the important factors in establishing dielectric-loss. On the other hand, the Q factors of MNT combinations would descend when the

holding time surpassed 4 h. This descend was signified that excessive grain growth also occurred at a longer holding time.
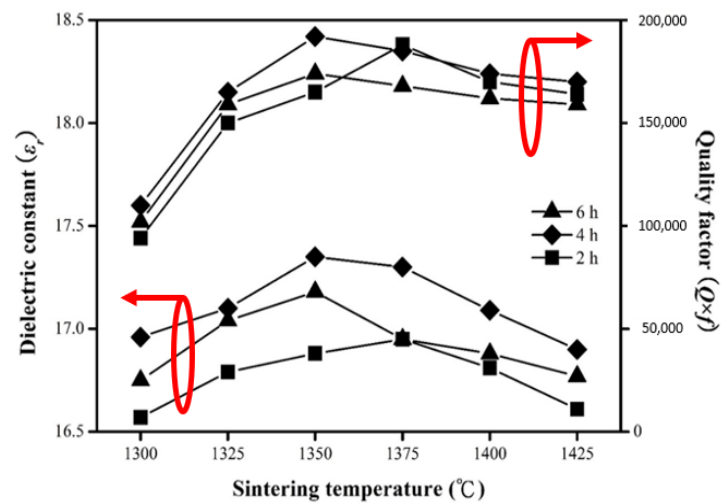

Figure 6. The dielectric constant and quality factor of the MNT ceramics as a function of the S.T. for varied holding time. The left and right circles with arrows Dielectric constant and Quality factor, respectively.

Figure 7 shows the temperature coefficients of resonant frequency (τ_f) of the MNT combinations with varied sintering conditions. The τ_f values were affiliated to the combination and the secondary phase of synthesized material in widespread. However, it seems to be closely related to the density of the proposed materials and sintering conditions. When the composition remained identical and no other secondary phases were observed, no remarkable variation in the τ_f value can be seen as anticipated. The measured τ_f values ranged from −45.2 to −51 ppm/°C as the specimen sintered at 1300 °C–1425 °C holding 4 h. At 1350 °C and holding 4 h, a τ_f value of −47 ppm/°C was obtained for the MNT combination.
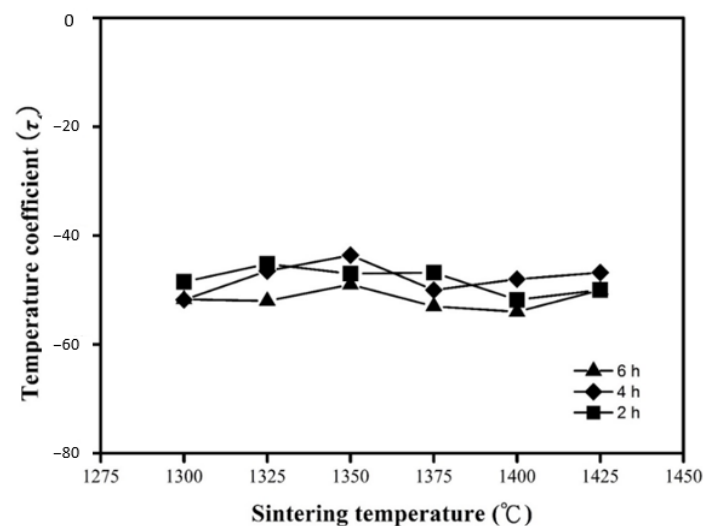

Figure 7. Dependence of τ_f value on sintering temperature of MNT ceramics for varied holding times.

3. Experimental Procedure

The specimen of MNT ceramics was merged with high-purity chemical powders. The stoichiometric percentages of raw oxide powders were weighted and ball-grinded in alcohol using zirconia balls as a grinding medium. Afterward, the blend solution was parched at 90 °C and

pre-sintered at 1100 °C holding 4 h. The pre-sintered powder was re-grinded in alcohol solution using zirconia balls and after parching, the polyvinyl alcohol was dropped into the powders as a binder and then crushed into a fine powder through a sieve. The gained powder was pressed into ingots under 100 MPa with 1 cm in diameter and 0.5 cm in thickness. The binder in these ingots was evaporated at 650 °C holding 2 h and then sintered at 1300–1425 °C for varied holding times as the heating rate of 10 °C/min.

The densities of ingots were measured and compute by using the Archimedes method. The permittivity and Q factor were measured using the Hakki–Coleman dielectric resonator methodology [29], as improved by Courtney [30]. The measurement system was connected to the Anritsu network analyzer with model MS46122B. The τ_f value was measured with an identical setup, but in the thermostat extent from 20 °C to 80 °C. The following formula was utilized to obtain the τ_f value (ppm/°C):

$$\tau_f = \frac{f_2 - f_1}{f_1(T_2 - T_1)}$$

where f_1 and f_2 represented the resonance frequencies at T_1 and T_2, respectively.

4. Conclusions

In this paper, the sintering conditions in $Mg_{0.95}Ni_{0.05}TiO_3$ ceramics and the influences on XRD analysis, microstructure, unit–cell constants, and microwave performance are systematically explored. The replacement of magnesium (Mg^{2+}) with nickel (Ni^{2+}) from 0.05 moles can form a $Mg_{0.95}Ni_{0.05}TiO_3$ solid solution, which can significantly reduce dielectric-loss. In particular, the pure $Mg_{0.95}Ni_{0.05}TiO_3$ combination possessed a high $Qf \sim 192{,}000$ (GHz), which represents an approximately 21.9% reduction in the dielectric loss compared with that of the pure $MgTiO_3$ and retained comparable ε_r (~17.35) and τ_f value (~−47 ppm/°C). A two-phase combination region was identified over the entire compositional range, and the existence of the $Mg_{0.95}Ni_{0.05}Ti_2O_5$ phase might diminish the dielectric performances of the example. The proposed dielectric combination, which has very low dielectric loss with appropriate permittivity and temperature characteristics, makes it a very promising candidate for practical applications in microwave and the communications systems of the new generation.

Author Contributions: Conceptualization, C.-H.S. and S.-H.L.; methodology, C.-H.S.; validation, C.-H.S., C.-L.P., and S.-H.L.; formal analysis, C.-H.S.; investigation, C.-H.S.; data curation, C.-L.P.; writing—original draft preparation, C.-H.S. and S.-H.L.; writing—review and editing, C.-L.P. and S.-H.L.; visualization, S.-H.L.; supervision, S.-H.L.; project administration, S.-H.L.; funding acquisition, S.-H.L. All authors have read and agreed to the published version of the manuscript.

Conflicts of Interest: The authors declare no conflict of interest.

References

1. Lin, S.H.; Chen, Y.B. Structure and characterization of B_2O_3 modified yNd($Mg_{1/2}Ti_{1/2}$)O_3-(1-y)$Ca_{0.8}Sr_{0.2}TiO_3$ ceramics with a near-zero temperature coefficient at microwave frequency. *Ceram. Int.* **2017**, *43*, 2368–2371. [CrossRef]
2. Nakagoshi, Y.; Sato, J.; Morimoto, M.; Suzuki, Y. Near-zero volume-shrinkage in reactive sintering of porous $MgTi_2O_5$ with pseudobrookite-type structure. *Ceram. Int.* **2016**, *42*, 9139–9144. [CrossRef]
3. Bor, B.; Heilmann, L.; Domènech, B.; Kampferbeck, M.; Vossmeyer, T.; Weller, H.; Schneider, G.A.; Giuntini, D. Mapping the Mechanical Properties of Hierarchical Supercrystalline Ceramic-Organic Nanocomposites. *Molecules* **2020**, *25*, 4790. [CrossRef]

4.   Palmero, P. Structural Ceramic Nanocomposites: A Review of Properties and Powders' Synthesis Methods. *Nanomaterials* **2015**, *5*, 656–696. [CrossRef]

5.   Freitas, A.E.; Manhabosco, T.M.; Batista, R.J.C.; Segundo, A.K.R.; Araújo, H.X.; Araújo, F.G.S.; Costa, A.R. Development and Characterization of Titanium Dioxide Ceramic Substrates with High Dielectric Permittivities. *Materials* **2020**, *13*, 386. [CrossRef]

6.   Itaalit, B.; Mouyane, M.; Bernard, J.; Womes, M.; Houivet, D. Effect of Post-Annealing on the Microstructure and Microwave Dielectric Properties of $Ba(Co_{0.7}Zn_{0.3})_{1/3}Nb_{2/3}O_3$ Ceramics. *Appl. Sci.* **2016**, *6*, 2. [CrossRef]

7.   Aljaafari, A.; Sedky, A. Influence of Fine Crystal Percentage on the Electrical Properties of ZnO Ceramic-Based Varistors. *Crystals* **2020**, *10*, 681. [CrossRef]

8.   Chen, Y.B.; Tseng, Z.L.; Chen, L.C.; Lin, C.C.; Miao, H.Y.; Li, J.H.; Lin, S.H. Crystal structure and microwave dielectric properties of $[(Mg_{0.6}Zn_{0.4})_{0.95}Co_{0.05}]_2TiO_4$-modified $Ca_{0.6}La_{0.8/3}TiO_3$ cordierite ceramics with a near-zero temperature coefficient. *J. Mater. Sci. Mater. Electron.* **2018**, *13*, 10709–10714. [CrossRef]

9.   Somiya, S. *Handbook of Advanced Ceramics*, 2nd ed.; Elsevier: Tokyo, Japan, 2013.

10. Sohn, J.H.; Inaguma, Y.; Yoon, S.O. Microwave Dielectric Characteristics of Ilmenite-Type Titanates with High Q Values. *Jpn. J. Appl. Phys.* **1994**, *33*, 5466. [CrossRef]

11. Chen, Y.C.; Su, C.F.; Weng, M.Z.; You, H.M.; Chang, K.C. Improvement microwave dielectric properties of Zn_2SnO_4 ceramics by substituting Sn^{4+} with Si^{4+}. *J. Mater. Sci. Mater. Electron.* **2014**, *25*, 2120. [CrossRef]

12. Shen, C.H.; Pan, C.L.; Lin, S.H. Structure, dielectric properties, and applications of $(Na_{0.5}Sm_{0.5})TiO_3$-modified $(Mg_{0.95}Ni_{0.05})TiO_3$ ceramics at microwave frequency. *Mater. Res. Bull.* **2015**, *169*, 65. [CrossRef]

13. Huang, C.L.; Wang, J.J. Dielectric Properties of Low Loss $(1–x)(Mg_{0.95}Zn_{0.05})TiO_3–xSrTiO_3$ Ceramic System at Microwave Frequency. *J. Am. Ceram. Soc.* **2007**, *90*, 858–862. [CrossRef]

14. Wang, H.P.; Yang, Q.; Li, D.; Huang, L.; Zhao, S.; Xu, S.D. Sintering Behavior and Microwave Dielectric Properties of $MgTiO_3$ Ceramics Doped with B_2O_3 by Sol-Gel Method. *J. Mater. Sci. Technol.* **2012**, *28*, 751. [CrossRef]

15. Wang, H.P.; Xu, S.Q.; Zhai, S.Y.; Deng, D.G.; Ju, H.D. Effect of B_2O_3 Additives on the Sintering and Dielectric Behaviors of $CaMgSi_2O_6$ Ceramics. *J. Mater. Sci. Technol.* **2010**, *26*, 351. [CrossRef]

16. Gakkai, D.T.; Gakkai, S.; Gakkai, T. *1976 Joint Convention Record of Four Institutes of Electrical Engineers*; Denki Shigakkai Jōchi Rengō Taikai Kikaku Iinkai: Tokyo, Japan, 1976.

17. Ferreira, V.M.; Azough, F.; Baptista, J.L.; Freer, R. DiC12: Magnesium titanate microwave dielectric ceramics. *Ferroelectrics* **1992**, *133*, 127. [CrossRef]

18. Ferreira, V.M.; Azough, F.; Freer, R. The effect of Cr and La on $MgTiO_3$ and $MgTiO_3$-$CaTiO_3$ microwave dielectric ceramics. *J. Mater. Res.* **1997**, *12*, 3293. [CrossRef]

19. Ferreira, V.M.; Baptista, J.L.; Kamba, S. Dielectric spectroscopy of $MgTiO_3$-based ceramics in the 109–1014Hz region. *J. Mater. Sci.* **1993**, *28*, 5894–5900. [CrossRef]

20. Huang, C.L.; Chen, Y.B. New dielectric material system of $Mg_{0.95}Co_{0.05}TiO_3 –Zn_{0.975}Ca_{0.025}TiO_3$ at microwave frequencies. *J. Alloys Compd.* **2009**, *477*, 712–715. [CrossRef]

21. Shen, C.H.; Huang, C.L. Microwave Dielectric Properties of $(Mg_{0.95}Ni_{0.05})TiO_3$-$SrTiO_3$ Ceramics with a Near-Zero Temperature Coefficient of Resonant Frequency. *Int. J. Appl. Ceram. Technol.* **2010**, *7*, 207–216.

22. Shen, C.H.; Huang, C.L. Microwave Dielectric Properties of $(1–x)(Mg_{0.95}Ni_{0.05})TiO_3–x(Ca_{0.8}Sr_{0.2})TiO_3$ Ceramic System With Near-Zero Temperature Coefficient. *Int. J. Appl. Ceram. Technol.* **2012**, *9*, 447–453. [CrossRef]

23. Liao, J.; Senna, M. Crystallization of titania and magnesium titanate from mechanically activated $Mg(OH)_2$ and TiO_2 gel mixture. *Mater. Res. Bull.* **1995**, *30*, 385. [CrossRef]

24. Huang, C.L.; Pan, C.L. Low-Temperature Sintering and Microwave Dielectric Properties of $(1–x)MgTiO_3–xCaTiO_3$ Ceramics Using Bismuth Addition. *J. Appl. Phys.* **2002**, *41*, 707. [CrossRef]

25. Shen, C.H.; Huang, C.L. Phase Evolution and Dielectric Properties of $(Mg_{0.95}M_{0.05}{}^{2+})$ Ti_2O_5 (M^{2+} = Co, Ni, and Zn) Ceramics at Microwave Frequencies. *J. Am. Ceram. Soc.* **2009**, *92*, 384–388.

26. Belous, A.; Ovchar, O.; Durilin, D. High-Q Microwave Dielectric Materials Based on the Spinel Mg_2TiO_4. *J. Am. Ceram. Soc.* **2006**, *89*, 3441–3445. [CrossRef]

27. Wang, J.J. Microwave dielectric properties of $(1–x)(Mg_{0.95}Zn_{0.05})TiO_3–x(Na_{0.5}La_{0.5})TiO_3$ ceramic system. *J. Alloys Compd.* **2009**, *486*, 423. [CrossRef]

28. Silverman, B.D. Microwave Absorption in Cubic Strontium Titanate. *Phys. Rev.* **1962**, *125*, 1921. [CrossRef]

29. Hakki, B.W.; Coleman, P.D. A Dielectric Resonator Method of Measuring Inductive Capacities in the Millimeter Range. *IEEE Trans. Microwave Theory Tech.* **1960**, *8*, 402. [CrossRef]

30. Courtney, W.E. Analysis and Evaluation of a Method of Measuring the Complex Permittivity and Permeability Microwave Insulators. *IEEE Trans. Microwave Theory Tech.* **1970**, *18*, 476. [CrossRef]

Sample Availability: Samples of the compounds are not available from the authors.